Int J Clin Exp Med 2019;12(5):4879-4887
www.ijcem.com /ISSN:1940-5901/IJCEM0089507

Original Article

HIF-1α shRNAs delivered by ultrasound-targeted cationic microbubble inhibit proliferation, migration, and invasion of ovarian cancer cells

Xiujuan Zhang[1], Zhikui Chen[1], Qingfu Qian[1], Leilei Liu[2], Ensheng Xue[1], Jing Yang[1], Bin Du[1], Dengke Hong[1], Qin Ye[1]

[1]Fujian Medical University Union Hospital, Fujian, China; [2]Second People's Hospital of Fujian Province, Fujian, China

Received December 6, 2018; Accepted April 10, 2019; Epub May 15, 2019; Published May 30, 2019

Abstract: Development of effective and safe treatment for ovarian cancer is urgent. In this study, a novel cationic microbubble was fabricated using the sonication method. The resulting microbubbles had a 27.5 ± 1.62 mV. surface zeta potential. They may greatly improve shRNA binding performance, achieving (10, 20, 30, 40, 50, and 60 μg) of DNA loading capacity per 5 × 10^8 microbubbles. Combined with these cationic microbubbles, HIF-1α-mediated gene delivery was evaluated. Gene transfection efficiency was optimized in CRL-2945™ and HTB-161™ cells. Knockdown of HIF-1α genes was successfully realized by HIF-1α-mediated shRNA transfection, resulting in HIF-1α-dependent protective effects on CRL-2945™ and HTB-161™ cells. Results indicated: (1) Ultrasound-targeted cationic microbubble-mediated shRNA transfection reduced expression levels of HIF-1α in ovarian cancer cells; (2) Ultrasound-targeted cationic microbubble-mediated shRNA transfection inhibited proliferation, migration, and invasion of ovarian cancer cells; and (3) Effects of HIF-1α shRNA transfection on tumor weight. In the current study, an ultrasound-targeted cationic microbubble system was established to successfully deliver shRNAs of HIF-1α, a key gene involved in the development and progression of ovarian cancer. HIF-1α shRNAs delivered by ultrasound-targeted cationic microbubbles can inhibit proliferation, migration, and invasion of ovarian cancer cells.

Keywords: Ovarian cancer, HIF-1α, ultrasound-targeted cationic microbubble, proliferation, migration, invasion

Introduction

A type of ovary malignancy with unacceptable high incidence and mortality rates, ovarian cancer seriously affects the health and quality of life of females [1]. In the United States, ovarian cancer is the tenth most common malignancy and a leading cause of cancer-related deaths among females [2]. Worldwide, ovarian cancer causes more than 140,000 deaths and affects more than 20,000 new patients every year [3]. Although treatments have been developed for ovarian cancer, surgical resection is still the only radical treatment for this disease [4, 5]. However, ovarian cancer, at early stages, is difficult to detect. Most patients are diagnosed at advanced stages and are not suitable for surgical operations [6]. Therefore, development of effective and safe treatment for ovarian cancer is urgent.

Gene targeted therapy has shown promising potential for treatment of different human diseases, including different types of cancer [7, 8]. An hypoxia-inducible factor, HIF-1α has been proven to be involved in nearly all aspects of development and progression of various types of human cancer [8, 9]. Inhibition of HIF-α has been shown to delay progression of certain types of cancer, including ovarian cancer [10, 11], indicating that inhibition of HIF-α expression may serve as a potential target for treatment of ovarian cancer. Short hairpin RNA (shRNA) transfection mediated by adenoviruses is an effective way to achieve RNA silencing. However, application of this technique has been limited by serious adverse effects [12]. There may be off-target effects and these shRNA could silence other unintended genes [13]. Recent studies have shown that shRNA transfection through ultrasound-targeted cationic mi-

crobubbles is safe and effective for treatment of hepatocellular carcinoma [14] and acute myocardial infarction [15].

Therefore, this technique may also be used to treat ovarian cancer via targeting HIF-1α.

Materials and methods

Preparation of ultrasound-targeted cationic microbubbles

Ultrasound-targeted cationic microbubbles were prepared, tested, and observed, according to the methods described by Sun et al. [14] and Zhang et al. [15]. Briefly, 1,2-distearoyl-sn-glycerol-3-phosphoethanolamine-N-[maleimide (polyethylene glycol)],3-[N-(N',N'-dimethyl-lamino-ethane)-carbamoyl] cholesterol (DC-CHOL), and 1,2-Dipalmitoyl-sn-glycero-3-phosphocholine (DPPC) were mixed, according to the molar proportion of 1:4:10, and dissolved in a laboratory flask. Organic solvent was removed using a rotary atmidometer under a high vacuum. The formation of a lipid film was observed. The mixture was dried overnight under a vacuum, followed by addition of phosphate-buffered saline (PBS), hydration on a rotary evaporator. and sonication with octafluoropropane gas (C3F8) gas using a sonicator (20 kHz, 33-42 W). Afterward, PBS was added to the solution containing per 5×10^8 microbubbles, adjusting the volume density 1×10^7 ml^{-1} of the cationic microbubbles. They were observed under a microscope. Size distribution, zeta potential, and concentration values were measured using the Zetasizer NANO ZS system (Malvern Instruments Ltd., Malvern, UK).

Binding of plasmids to microbubbles

HIF-1α MISSION® shRNA EGFP Plasmid DNA (SHCLND-NM_001530, Sigma-Aldrich) and a plasmid containing EGFP only were used. Different amounts of plasmid DNA (10, 20, 30, 40, 50, and 60 μg) were mixed with 5×10^8 microbubbles. This was followed by incubation for 10 minutes. Afterward, the mixture was centrifuged (1,000 × g) for 15 minutes, making two separated layers. The lower clear layer containing unbound DNA was collocated and DNA concentrations were measured using spectrophotometry. The upper layer was collected and stained with SYBR Gold. The plasmid-microbubble complex was observed under a fluorescence microscope.

Cell lines and cell culturing

Human ovarian cancer cell lines CRL-2945™ and HTB-161™ were purchased from ATCC (USA). Cell culturing was performed according to manufacturer instructions. Cells were harvested during the logarithmic growth phase for subsequent experiments.

Ultrasound-targeted cationic microbubble and Lipofectamine-mediated shRNA transfection

The cells were transferred to 24-well plates with 4×10^4 cells per well and cultured overnight, reaching 70-80% confluence. The combination of 30 μg of the plasmid and 5×10^8 microbubbles reached the maximum binding efficiency. Therefore, 15 μg of the plasmid and 5×10^8 microbubbles were mixed and added into each well. After incubation for 15 minutes, the plates were treated with 1.0 W/cm^2 ultrasound power for 15 seconds [15]. Moreover, Lipofectamine 2000 (11668-019, Invitrogen, Carlsbad, USA) was used to transfect 15 μg of the vector into the same number of cells.

Real-time quantitative PCR

Total RNA was extracted from cells using TRIzol Reagent (Invitrogen, USA). RNA quality was checked. Only RNA samples with an A260/A280 ratio between 1.8 and 2.0 were used in reverse transcription to synthesize cDNA. The following primers were used in PCR reactions: 5'-AGCCCTAGATGGCTTTGTGA-3' (forward) and 5'-TATCGAGGCTGTGTCGACTG-3' (reverse) for HIF-1α; 5'-GACCTCTATGCCAACACAGT-3' (forward) and 5'-AGTACTTGCGCTCAGGAGGA-3' (reverse) for β-actin. PCR reaction conditions were: 95°C for 37 seconds, followed by 40 cycles of 95°C for 15 seconds and 60°C for 32 seconds. Ct values were analyzed using the $2^{-\Delta\Delta CT}$ method and relative expression levels of HIF-1α were normalized to endogenous control β-actin.

Cell proliferation assay

The cells were seeded into 96-well plates with 5×10^3 cells per well and cultured. Next, 10 μL of CCK-8 was added at 24, 48, 72, and 96 hours. After the addition of CCK-8 solution, the cells were incubated for another 3 hours. OD values at 450 nm were measured using a microplate reader. Cell proliferation was normalized to the control group (set to 100).

Table 1. Characteristics of microbubbles

Mean diameter (μm)	Concentration (× 10^9/ml)	Zeta potential (mV)
3.01 ± 0.42	3.14 ± 0.31	27.5 ± 1.62

Cell migration and invasion assay

Cell migration ability was measured by Transwell cell migration assays (BD Biosciences, USA). Briefly, 5 × 10^3 cells were transferred to the upper chamber, while RPMI-1640 medium (Thermo Fisher Scientific, USA) containing 20% FCS (Sigma-Aldrich, USA) was added to the lower chamber. Membranes were collected 24 hours later. This was followed by staining with 0.5% crystal violet (Sigma-Aldrich, USA) for 15 minutes. Stained cells were counted under an optical microscope (Olympus, Japan). Before cell invasion assays, the upper chamber was precoated with Matrigel (356234, Millipore, USA). Cell migration and invasion were normalized to the control group (set to 100).

Western blotting

Total protein was extracted from cells and quantified using the BCA method. Protein samples were then subjected to 10% SDS-PAGE gel electrophoresis, using 30 μg of protein from each sample. Afterward, proteins were transferred to PVDF membranes under 25 V for 30 minutes. The membranes were blocked with 5% skimmed milk, washed with TBST, and incubated with primary antibodies, including rabbit anti-HIF-1α (1:2000, ab61608, Abcam) and anti-β-actin primary antibody (1:1000, ab8226, Abcam), overnight at 4°C. The next day, the membranes were washed with PBS and further incubated with anti-rabbit IgG-HRP secondary antibody (1:1000, MBS435036, MyBioSource) at room temperature for 1 hour. After washing, signals were detected the using ECL (Sigma-Aldrich, USA) method. Relative expression levels of HIF-1α were normalized to endogenous control β-actin using Image J, measuring optical densities (ODs) of the band.

Mice transplantation

Thirty nude mice (20 ± 2 g) were obtained from Guangdong Medical Laboratory Animal Center (Guangdong, China). They were randomly divided in three groups, with 10 mice in each group. Next, 10^6 cells of CRL-2945™ cell line were transfected with ultrasound-targeted cationic microbubble or Lipofectamine overexpression cell line. Also, cells without any transfection were resuspended in 100 μL of the Matrigel/PBS mixture and subcutaneously injected into the back of each mice. The mice were sacrificed 4 weeks after transplantation. Weight and volume levels of the tumors were measured. These animal experiments were approved by the Ethics Committee of Fujian Medical University Union Hospital.

Statistical analysis

Statistical analysis was performed using GraphPad software. Comparisons of measurements among groups were performed using one-way ANOVA, followed by post-hoc Bonferroni's test. $P < 0.05$ indicates statistically significant differences.

Results

Characteristics of microbubbles alone and the plasmid-microbubble complex

Characteristics of microbubbles in suspension were detected. As shown in **Table 1**, the mean diameter of the microbubbles was 3.01 ± 0.42 μm. The concentration of microbubbles in suspension was 3.14 ± 0.31 × 10^9/mL and the mean Zeta potential was 27.5 ± 1.62 mV. Observation under an optical microscope showed that the plasmid-microbubble complexes were uniformly distributed with a round shape. Green fluorescence could be observed under a fluorescence microscope (**Figure 1**).

Ultrasound-targeted cationic microbubble-mediated shRNA transfection reduced expression levels of HIF-1α in ovarian cancer cells

After transfection, expression of HIF-1α in human ovarian cancer cell lines CRL-2945™ and HTB-161™ was detected using qRT-PCR and Western blot at mRNA and protein levels, respectively. Compared with non-transfected cells (control, C) and cells transfected with EGFP-only-plasmid (negative control, NC), expression levels of HIF-1α were significantly reduced in cells transfected with HIF-1α shRNA, through both ultrasound-targeted cationic microbubbles and Lipofectamine 2000 ($p < 0.05$) (**Figure 2A**). In addition, expression levels of HIF-1α were significantly lower in cells transfected with

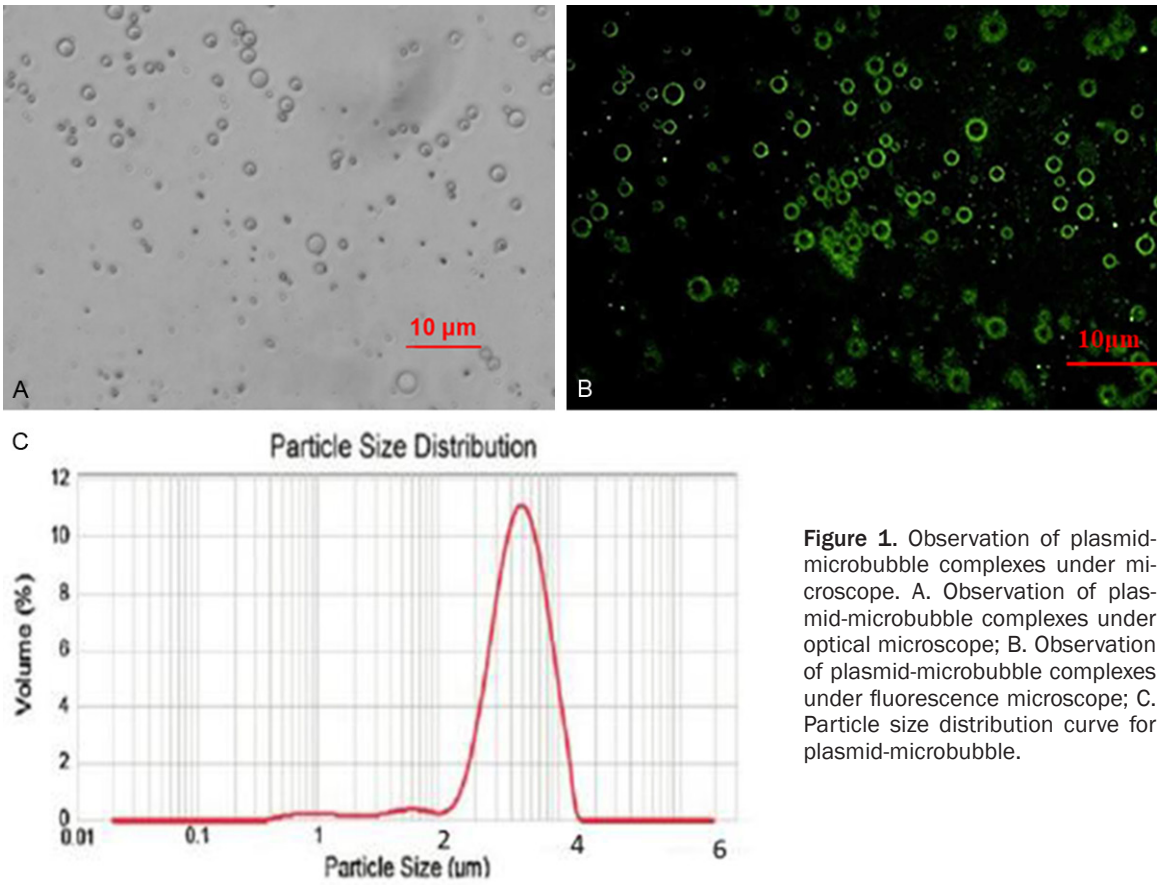

Figure 1. Observation of plasmid-microbubble complexes under microscope. A. Observation of plasmid-microbubble complexes under optical microscope; B. Observation of plasmid-microbubble complexes under fluorescence microscope; C. Particle size distribution curve for plasmid-microbubble.

ultrasound-targeted cationic microbubbles than in cells transfected with Lipofectamine 2000 ($p < 0.05$). Similarly, expression levels of HIF-1α protein were significantly reduced after transfection with HIF-1α shRNA (**Figure 2B**, $p < 0.05$). Present data suggests that ultrasound-targeted cationic microbubble-mediated shRNA transfection can effectively reduce expression levels of HIF-1α in ovarian cancer cells.

Ultrasound-targeted cationic microbubble-mediated shRNA transfection inhibited proliferation, migration, and invasion of ovarian cancer cells

CCK-8 cell proliferation assays were performed to measure cell proliferation ability after ultrasound-targeted cationic microbubble-mediated HIF-1α shRNA transfection. Compared with control cells and negative control cells, the proliferation ability of human ovarian cancer cell lines CRL-2945™ and HTB-161™ was significantly reduced after HIF-1α shRNA transfection. Transwell cell migration assays were carried out to measure cell migration ability after ultrasound-targeted cationic microbubble-mediated HIF-1α shRNA transfection (**Figure 3**). Compared with control cells and negative control cells, the migration ability of human ovarian cancer cell lines CRL-2945™ and HTB-161™ was significantly reduced after HIF-1α shRNA transfection. Transwell cell invasion assays were carried out to measure cell invasion ability after ultrasound-targeted cationic microbubble-mediated HIF-1α shRNA transfection (**Figure 4**). Compared with control cells and negative control cells, the invasion ability of human ovarian cancer cell lines CRL-2945™ and HTB-161™ was significantly reduced after HIF-1α shRNA transfection. Current data suggests that ultrasound-targeted cationic microbubble-mediated HIF-1α shRNA transfection can effectively inhibit ovarian cell proliferation, migration, and invasion (**Figure 5**).

Effects of HIF-1α shRNA transfection on tumor weights

Weights of tumors derived from cells with HIF-1α shRNA transfection through ultrasound-targeted cationic microbubbles and Lipofectamine 2000 on tumor growth were lower than tumors

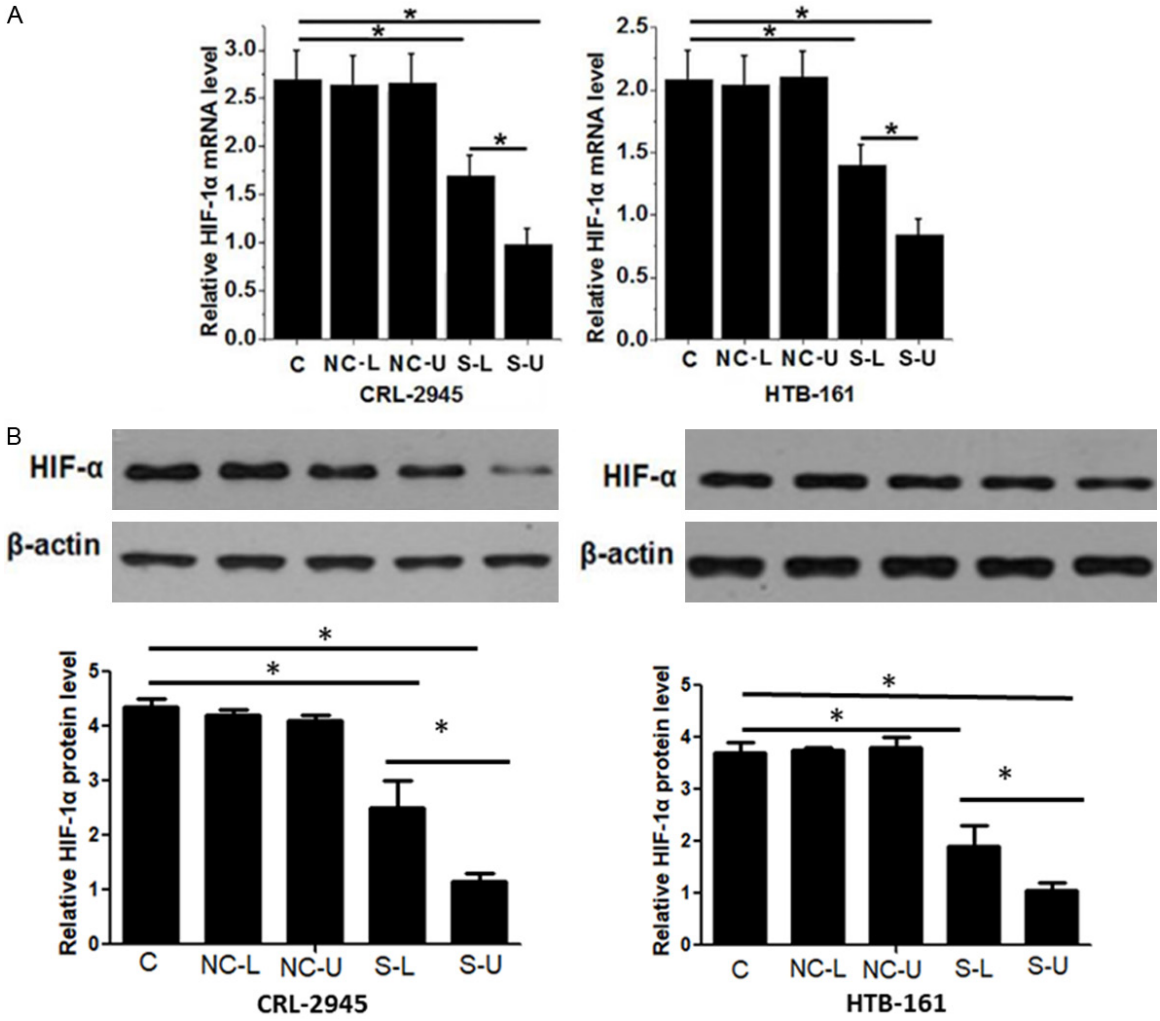

Figure 2. Ultrasound-targeted cationic microbubble-mediated shRNA transfection reduced expression levels of HIF-1α in ovarian cancer cells. A. Expression of HIF-1α mRNA in different ovarian cancer cell lines with different treatments; B. Expression of HIF-1α protein in different ovarian cancer cell lines with different treatments. Notes: *, $p < 0.05$; Control: C, NC-U, negative control of transfection through ultrasound-targeted cationic microbubble; NC-L, negative control of transfection through Lipofectamine 2000; S-U, transfection of HIF-1α shRNA through ultrasound-targeted cationic microbubble; S-L, transfection of HIF-1α through Lipofectamine 2000.

derived from cells without transfection ($p < 0.05$) (**Figure 6**). In addition, weights of tumors derived from cells with HIF-1α shRNA transfection through ultrasound-targeted cationic microbubbles were significantly lower than tumors derived from cells with HIF-1α shRNA transfection through Lipofectamine 2000 ($p < 0.05$). This further confirmed the higher knockdown efficiency of HIF-1α shRNA delivered by ultrasound-targeted cationic microbubbles, compared to Lipofectamine 2000.

Discussion

Development and progression of ovarian cancer is a complex process, with various internal and external factors involved. Hypoxia-inducible factor 1α, also known as HIF-1α, is a subunit of a transcription factor hypoxia-inducible factor 1 [16]. Numerous studies have shown that abnormal expression of HIF-1α, caused by genetic alternations or hypoxia, is closely correlated with expression of various types of human cancer [17]. In the study of gastric cancer, Wang et al. [18] reported that HIF-1α was usually overexpressed in gastric tumor tissues. They also showed that HIF-1α overexpression triggered abnormal expression of a gene network, promoting the progression of cancer. In another study, Saponaro found that HIF-1α expression could contribute to the formation of new tumor tissues. This, in turn, sped up the

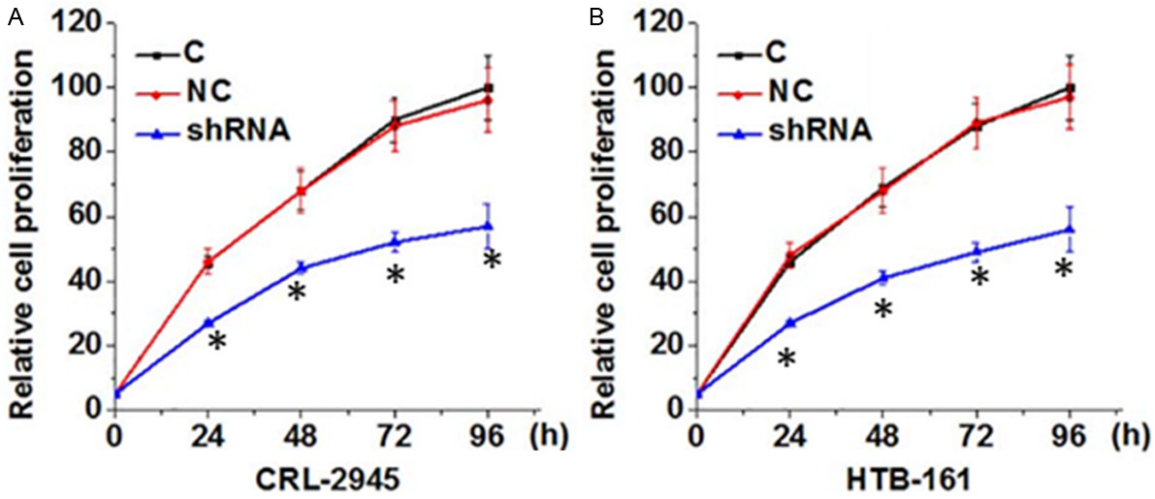

Figure 3. Ultrasound-targeted cationic microbubble-mediated shRNA transfection inhibited proliferation of ovarian cancer cells. A. Relative cell proliferation of CRL-2945 ovarian cancer cells. B. Relative cell proliferation of HTB-161 ovarian cancer cells. Notes: *, $p < 0.05$ for between group comparisons at the same time point.

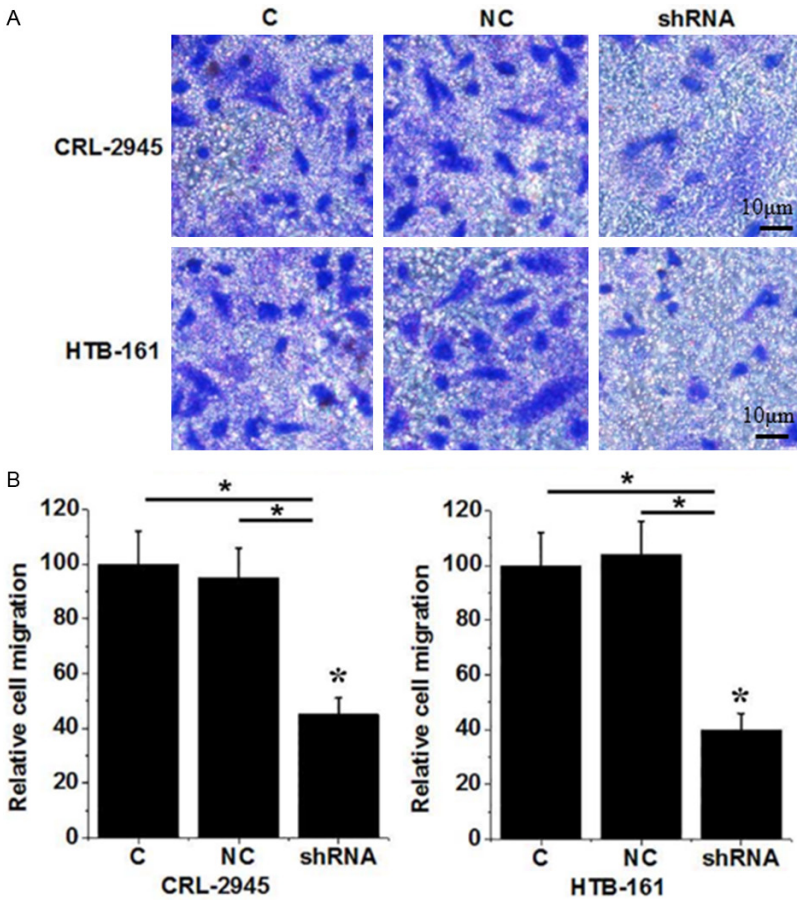

Figure 4. Ultrasound-targeted cationic microbubble-mediated shRNA transfection inhibited migration of ovarian cancer cells. A. Representative images of Transwell cell migration assays; B. Normalized cell migration abilities. Notes: *, $p < 0.05$.

growth of tumors [19]. Increased expression levels of HIF-1α have been observed in patients with ovarian cancer. HIF-1α overexpression in ovarian cancer tissues has been shown to promote the development and progression of cancer and induce drug resistance, leading to poor treatment outcomes [20]. In contrast, inhibition of HIF-α has been shown to delay progression ovarian cancer [11]. Therefore, HIF-1α expression silencing may be a potential method of improving conditions of patients with ovarian cancer.

RNA interference is a gene silencing method that can inhibit gene expression at a post-transcriptional level. Thus, siRNA silencing is a widely used method for gene expression regulation. However, the effects only last for several days due to the short half-life. Compared with siRNA, transfection of shRNA can achieve

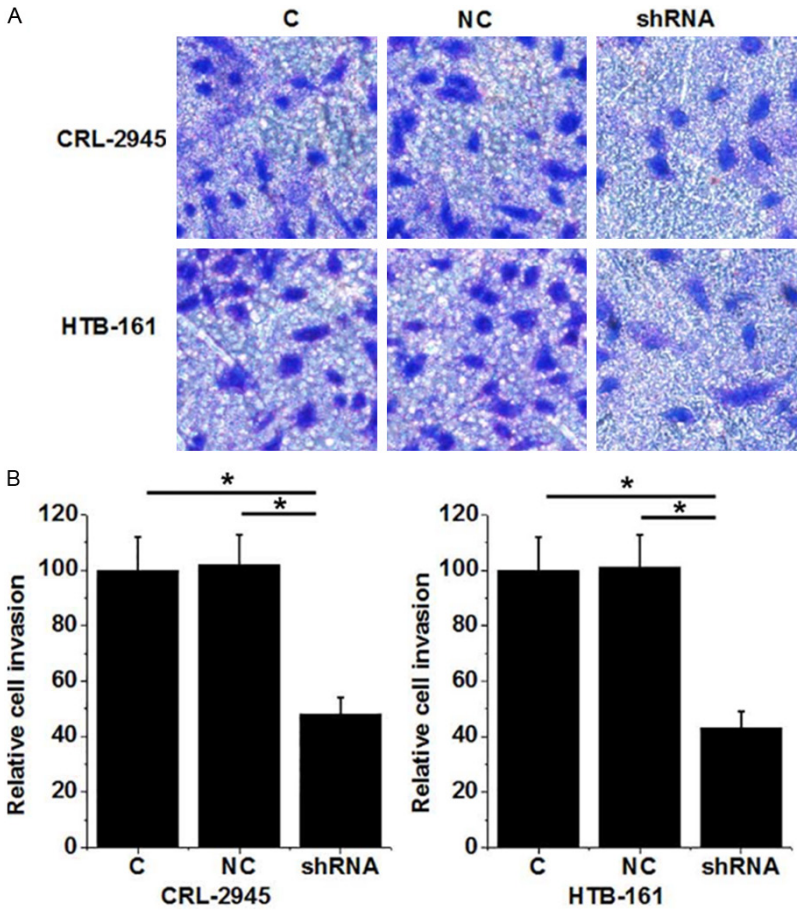

Figure 5. Ultrasound-targeted cationic microbubble-mediated shRNA transfection inhibited invasion of ovarian cancer cells. A. Representative image of Transwell cell invasion assays; B. Normalized cell invasion ability. Notes: *, $p < 0.05$.

longer effects (several weeks or even longer) through sustainable production of siRNA with the actions of Dicer enzymes. Currently, a variety of different gene delivery methods have been developed to achieve RNA silencing [21]. However, the application of those techniques has been limited by either low efficiency or adverse effects [22]. Recent studies have shown that shRNA transfection through ultrasound-targeted cationic microbubble is a safe and effective method for treatment of ischemic myocardium [14] and acute myocardial infarction [15]. In this study, this technique was used to deliver shRNA to two ovarian cancer cell lines, targeting HIF-1α. As a result, high silencing efficiencies were achieved.

HIF-1α expression affects proliferation, migration, and invasion of various types of cancer. In a study of non-small cell lung cancer, Zhou et al. proved that HIF-1α overexpression was responsible for enhanced proliferation, migration, and invasion of cancer cells [23]. In another study, HIF-1α knockdown in malignant gliomas significantly inhibited migration and invasion of cancer cells [24]. Consistent with previous studies, in this study, significantly increased proliferation, migration, and invasion abilities were observed in two ovarian cancer cell lines after ultrasound-targeted cationic microbubble-mediated HIF-1α shRNA transfection. Current data suggests that ultrasound-targeted cationic microbubble-mediated HIF-1α shRNA transfection can inhibit proliferation, migration, and invasion of ovarian cancer cells.

It is noteworthy that HIF-1α is also involved in the regulation of cell proliferation of many normal cell lines [25]. Thus, the use of HIF-1α as a target for cancer treatment may rely on accurate drug delivery. Animal experiments were performed using cancer cells, pretreated *in vitro* with microbubbles with anti HIF-1α shRNA. This cannot be used to mimic *in vivo* conditions. Short circulation times and huge particle sizes are still the biggest challenges in the clinical application of this technique.

Sonoporation harbors complicated aspects. Gene transfer efficiency levels are low with sonoporation. Moreover, 37.5-50 μg of the plasmid should be applied to a single rat with sonoporation *in vivo* [26]. This limitation is one of the reasons that sonoporation has not been applied clinically, as mentioned above. Another limitation is cell damage caused with sonoporation. Miller et al. [27] irradiated cells with 2.25 MHz continuous ultrasound for 1 minute. When an ultrasound contrast agent (Definity, a Perflutren lipid microsphere injectable suspension; Bristol Myers Squibb Medical Imaging, N. Billerica, MA) was added to the culture media, the

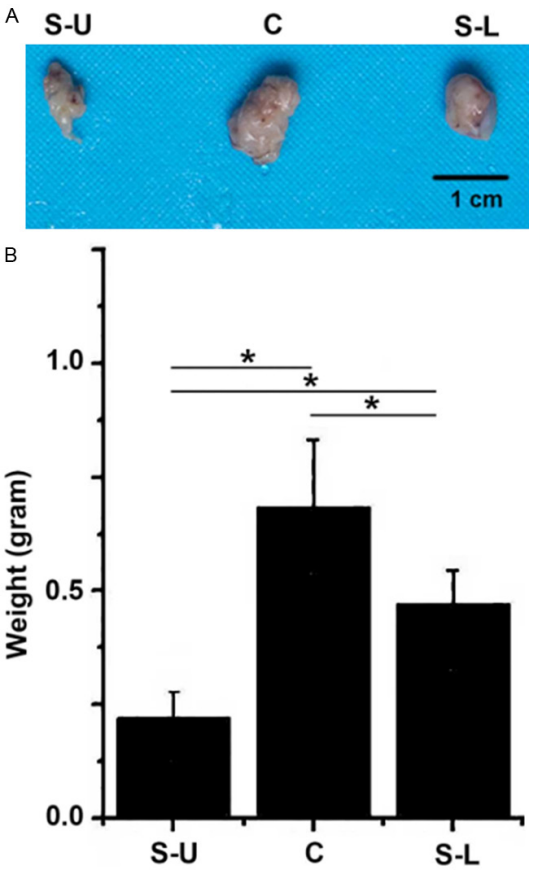

Figure 6. Comparisons of weights of tumors derived from cells transfected with HIF-1α shRNA through ultrasound-targeted cationic Microbubble and Lipofectamine 2000. A. Representative image of tumors derived from different cell group; B. Normalized weights of the tumors from different cell groups. Notes: *, $p < 0.05$; NC-U, negative control of transfection through ultrasound-targeted cationic microbubble; NC-L, negative control of transfection through Lipofectamine 2000; S-U, transfection of HIF-1α shRNA through ultrasound-targeted cationic microbubble; S-L, transfection of HIF-1α through Lipofectamine 2000.

irradiated cells underwent apoptosis. Enzymatic activity and mitochondrial membrane are also changed after sonoporation. Stress to the endoplasmic reticulum and mitochondria triggers apoptosis [28]. Sonoporation delays DNA synthesis, arresting cell cycle [29]. It should be noted that sonoporation itself may cause apoptosis when applied to cancer with therapeutic genes [30].

In conclusion, an ultrasound-targeted cationic microbubble system was established to deliver HIF-1α shRNA to ovarian cells. Satisfactory silencing efficiency was achieved. In addition, HIF-1α shRNA silencing mediated by ultrasound-targeted cationic microbubble led to significantly inhibited proliferation, migration, and invasion abilities of ovarian cancer cells. The current study provides reference for the clinical application of this technique. Future studies will include *in vivo* assays, testing the safety of this method.

Acknowledgements

This work was supported by the Joint Health Fund Project of Fujian Natural Fund (2015J01468), Youth Foundation Project of Fujian Provincial Health and Family Planning Commission (2013-1-25), and Emergency Management Project of National Natural Science Foundation of China (81550039).

Disclosure of conflict of interest

None.

Address correspondence to: Qin Ye, Fujian Medical University Union Hospital, No. 29 Xinquan Road, Fuzhou 350001, Fujian, China. Tel: +86-13365910586; E-mail: jenifer81@126.com

References

[1] Center MM, Jemal A, Lortet-Tieulent J, Ward E, Ferlay J, Brawley O and Bray F. International variation in prostate cancer incidence and mortality rates. Eur Urol 2012; 61: 1079-1092.

[2] Risch HA, Mclaughlin JR, Cole DE, Rosen B, Bradley L, Kwan E, Jack E, Vesprini DJ, Kuperstein G and Abrahamson JL. Prevalence and penetrance of germline BRCA1 and BRCA2 mutations in a population series of 649 women with ovarian cancer. Am J Hum Genet 2001; 68: 700-710.

[3] Ahmedin J, Freddie B, Center MM, Jacques F, Elizabeth W and David F. Global cancer statistics. Ca Cancer J Clin 2011; 61: 69-90.

[4] Pujade-Lauraine E, Hilpert F, Weber B, Reuss A, Poveda A, Kristensen G, Sorio R, Vergote I, Witteveen P and Bamias A. AURELIA: a randomized phase III trial evaluating bevacizumab combined with chemotherapy for platinum-resistant recurrent ovarian cancer. J Clin Oncol 2012; 30: 327s.

[5] Sheets NC, Goldin GH, Meyer A-M, Wu Y, Chang Y, Stürmer T, Holmes JA, Reeve BB, Godley PA and Carpenter WR. Intensity-modulated radiation therapy, proton therapy, or conformal radiation therapy and morbidity and disease control in localized prostate cancer. JAMA 2012; 307: 1611-1620.

[6] Rauh-Hain JA, Krivak TC, Del Carmen MG and Olawaiye AB. Ovarian cancer screening and early detection in the general population. Rev Obstet Gynecol 2011; 4: 15-21.
[7] Ross JS, Fletcher JA, Bloom KJ, Linette GP, Stec J, Symmans WF, Pusztai L and Hortobagyi GN. Targeted therapy in breast cancer: the HER-2/neu gene and protein. Mol Cell Proteomics 2004; 3: 379-398.
[8] Castello R, Borzone R, D'Aria S, Annunziata P, Piccolo P and Brunettipierri N. Helper-dependent adenoviral vectors for liver-directed gene therapy of primary hyperoxaluria type 1. Gene Ther 2016; 23: 129-134.
[9] Xiang L, Gilkes DM, Hu H, Luo W, Bullen JW, Liang H and Semenza GL. HIF-1α and TAZ serve as reciprocal co-activators in human breast cancer cells. Oncotarget 2015; 6: 11768-11778.
[10] Chen J, Ding Z, Peng Y, Pan F, Li J, Zou L, Zhang Y and Liang H. HIF-1α Inhibition reverses multidrug resistance in colon cancer cells via downregulation of MDR1/P-glycoprotein. PLoS One 2014; 9: e98882.
[11] Yeh YM, Chuang CM, Chao KC and Wang LH. MicroRNA-138 suppresses ovarian cancer cell invasion and metastasis by targeting SOX4 and HIF-1α. Int J Cancer 2013; 133: 867-878.
[12] Muroi Y, Ru F, Chou YL, Carr MJ, Undem BJ and Canning BJ. Selective inhibition of vagal afferent nerve pathways regulating cough using NaV 1.7 shRNA silencing in guinea pig nodose ganglia. Am J Physiol Regul Integr Comp Physiol 2013; 304: R1017-R1023.
[13] Moses J, Goodchild A and Rivory LP. Intended transcriptional silencing with siRNA results in gene repression through sequence-specific off-targeting. RNA 2010; 16: 430-441.
[14] Xue Y, Yang G, Wang C, Li X and Du G. Effects of shRNA-mediated SOX9 inhibition on cell proliferation and apoptosis in human HCC cell line Hep3B mediated by ultrasound-targeted microbubble destruction (UTMD). Cell Biochem Biophys 2015; 73: 553-558.
[15] Li Z, Sun Z, Ren P, You M, Jing Z, Fang L, Jing W, Chen Y, Fei Y and Zheng H. Localized delivery of shRNA against PHD2 protects the heart from acute myocardial infarction through ultrasound-targeted cationic microbubble destruction. Theranostics 2017; 7: 51-66.
[16] Semenza G, Rue E, Iyer N, Pang M and Kearns W. Assignment of the hypoxia-inducible factor 1α gene to a region of conserved synteny on mouse chromosome 12 and human chromosome 14q. Genomics 1996; 34: 437-439.
[17] Semenza GL. Targeting HIF-1 for cancer therapy. Nat Rev Cancer 2003; 3: 721-732.
[18] Wang J, Ni Z, Duan Z, Wang G and Li F. Altered expression of hypoxia-inducible factor-1α (HIF-1α) and its regulatory genes in gastric cancer tissues. PLoS One 2014; 9: e99835.
[19] Saponaro C, Malfettone A, Ranieri G, Danza K, Simone G, Paradiso A and Mangia A. VEGF, HIF-1α expression and MVD as an angiogenic network in familial breast cancer. PLoS One 2013; 8: e53070.
[20] Donato MD, Fanelli M, Mariani M, Raspaglio G, Pandya D, He S, Fiedler P, Petrillo M, Scambia G and Ferlini C. Nek6 and Hif-1α cooperate with the cytoskeletal gateway of drug resistance to drive outcome in serous ovarian cancer. Am J Cancer Res 2015; 5: 1862.
[21] Zhang CQ, Bradshaw JD, Whitham SA and Hill JH. The development of an efficient multipurpose bean pod mottle virus viral vector set for foreign gene expression and RNA silencing. Plant Physiol 2010; 153: 52-65.
[22] Voinnet O. Induction and suppression of RNA silencing: insights from viral infections. Nat Rev Genet 2005; 6: 206-220.
[23] Zhou C, Ye L, Jiang C, Bai J, Chi Y and Zhang H. Long noncoding RNA HOTAIR, a hypoxia-inducible factor-1α activated driver of malignancy, enhances hypoxic cancer cell proliferation, migration, and invasion in non-small cell lung cancer. Tumour Biol 2015; 36: 9179-9188.
[24] Fujiwara S, Nakagawa K, Harada H, Nagato S, Furukawa K, Teraoka M, Seno T, Oka K, Iwata S and Ohnishi T. Silencing hypoxia-inducible factor-1α inhibits cell migration and invasion under hypoxic environment in malignant gliomas. Int J Oncol 2007; 30: 793-802.
[25] Hubbi ME and Semenza GL. Regulation of cell proliferation by hypoxia-inducible factors. Am J Physiol Cell Physiol 2015; 309: C775-C782.
[26] Panje CM, Wang DS, Pysz MA, Paulmurugan R, Ren Y, Tranquart F, Tian L and Willmann JK. Ultrasound-mediated gene delivery with cationic versus neutral microbubbles: effect of DNA and microbubble dose on in vivo transfection efficiency. Theranostics 2012; 2: 1078-1091.
[27] Miller DL and Quddus J. Sonoporation of monolayer cells by diagnostic ultrasound activation of contrast-agent gas bodies. Ultrasound Med Biol 2000; 26: 661-667.
[28] Zhong W, Sit WH, Wan JM and Yu AC. Sonoporation induces apoptosis and cell cycle arrest in human promyelocytic leukemia cells. Ultrasound Med Biol 2011; 37: 2149-2159.
[29] Chen X, Wan JM and Yu AC. Sonoporation as a cellular stress: induction of morphological repression and developmental delays. Ultrasound Med Biol 2013; 39: 1075-1086.
[30] Miller DL and Dou CY. Induction of apoptosis in sonoporation and ultrasonic gene transfer. Ultrasound Med Biol 2009; 35: 144-154.